International Journal of
Clinical Cardiology & Research

Review Article

Magnetic Resonance Imaging in Coronary Interventions and Myocardial Microinfarction -

Maythem Saeed* and Mark W. Wilson

Department of Radiology and Biomedical Imaging, School of Medicine, University of California San Francisco, San Francisco, USA

***Address for Correspondence:** Maythem Saeed, Department of Radiology and Biomedical Imaging, University of California San Francisco, 185 Berry Street, Suite 350, Campus Box 0946, San Francisco, CA 94107-5705, USA, Tel: +415-514-6221; Fax : +415-353-9423; E-mail: Maythem.Saeed@ucsf.edu

Submitted: 27 January 2017; **Approved:** 09 February 2017; **Published:** 13 February 2017

Citation this article: Saeed M, Wilson MW. Magnetic Resonance Imaging in Coronary Interventions and Myocardial Microinfarction. Int J Clin Cardiol Res. 2017;1(1): 031-042.

ABSTRACT

Coronary Artery Bypass Grafting (CABG) and Percutaneous Coronary Intervention (PCI) were introduced in 1968 and 1977, respectively. Currently these procedures are used for the treatment of ischemic heart disease. The procedures are safe and can achieve effective relief of coronary arterial obstruction in 90% to 95% of patients. Other investigators also found these procedures often generate macro- and micro-emboli resulting in additional damage. A recent SYNTAX trial showed that the rates of myocardial infarction and death at 1 year were similar between patients who underwent CABG and those who underwent PCI. Unlike Doppler sonography, Magnetic Resonance Imaging (MRI) has not been used for counting circulating coronary micro-emboli during coronary interventions. On the other hand, MRI provides valuable information on coronary artery anatomy, cardiac function, myocardial perfusion and viability. It also has the potential to reliably assess the beneficial effects of new therapies. However, the detection of myocardial microinfarct micro-emboli in patients is still challenging, because of the large variability in the volumes/sizes of dislodged micro-emboli and microinfarct sizes after coronary interventions. The spatial resolution of MR scanners and relaxivity of contrast media play important role in visualizing microinfarct. Recent clinical and preclinical techniques were able to count coronary micro-emboli and demonstrate myocardial microinfarct. These studies shed light on the complex relationship between coronary interventions and myocardial microinfarct. Preclinical studies, however, indicated that delayed contrast enhanced MRI underestimates microinfarct size compared with histopathology. Recent studies revealed that micro-emboli were cleared from the vasculature compartment by either hemodynamic pressure or angiography. The ability to detect, characterize and size intraoperative occurring coronary emboli, using non-invasive imaging techniques, may have a great potential for patient's safety. At this time, there are no known drugs/device that have demonstrated conclusively myocardial protection.

Keywords: Coronary interventions; MRI; Coronary microembolization; Myocardial infarct; Cardiac function

INTRODUCTION

The causes of myocardial infarction are coronary spasm, spontaneous clot formation, dislodgment of atherosclerotic plaques in major coronary arteries, stent thrombosis, thrombi from atrial fibrillation, thrombi from cardiopulmonary bypass, etc [1]. *P*ercutaneous Coronary Intervention (PCI) or Coronary Artery Bypass Grafting (CABG) procedures have been used to vascularize obstructed major coronary arteries, reduce myocardial infarct size; improve Left Ventricular (LV) function and clinical outcome. Paradoxically, revascularization of infarct-related coronary artery could produce further myocardial damage to previously undamaged myocardium by a phenomenon called reperfusion injury or coronary microembolization [2-4]. Thus, coronary intervention can protect and harm the heart. Several studies have emphasized the ubiquitous occurrence of distal embolization of atheromatous and thrombotic debris after coronary intervention, potentially resulting in microcirculatory dysfunction, abnormal myocardial metabolism, and additional necrosis [5-7]. Cuculi, et al. [4] showed that 5 - 30% of the patients suffered from coronary embolization after PCI and the effects on myocardium varied from non-symptomatic to sudden death [8-10]. A recent SYNTAX trial showed that the rates of death and myocardial infarction at 1 year were similar between patients who underwent CABG and those who underwent PCI; whereas the rate of stroke was increased in the CABG group and the rate of repeat revascularization was increased in the PCI group [11].

Delayed contrast enhanced MRI (DE-MRI) sequences can reliably measure the size and transmurality of acute and chronic Myocardial Infarct (MI). However, these imaging sequences have in many cases limitation in visualizing myocardial microinfarct since the level of signal enhancement and thresholding methods to delineate micro-damage are insufficient, thus DE-MRI should be used with other imaging biometrics, such as cardiac perfusion and function. This review focuses on clinical and preclinical studies that addressed coronary micro-emboli and their effects on cardiac function, perfusion and viability.

Coronary emboli

Coronary embolization describes a process where aggregated dislodged platelets, atherothrombotic debris and released vasoactive substances induce micro vascular obstruction, oxidative stress, inflammation and patchy microinfarction. Troncoso, et al. [12] found an association between coronary artery disease and cerebral microinfarct. Most autopsy-based studies discussed to this point are cross-sectional and therefore limited in their ability to explore the incidence and consequences of microinfarct. An autopsy-based study, however, showed that coronary embolization occurred 3 to 4 times more often in the left coronary artery than in the right, and in the Left Anterior Descending (LAD) than in the left circumflex [13]. It is reasonable to surmise that location and number of microinfarct determine the clinical impact. The middle range of coronary microemboli retrieved after coronary intervention was 47-2503 μm.

Cardiac injury biomarkers

Cardiac injury occurs when there is disruption of myocyte membrane integrity, that results in the loss of intracellular constituents, such as creatine kinase, troponin, myoglobin, heart-type fatty acid binding protein, and lactate dehydrogenase. In an experimental study [14], investigators found that the increases in creatine-kinase MB and troponin I depend on the volume of microemboli and time of blood sampling.

Cardiologists documented the increase of plasma cardiac injury biomarkers after PCI [15,16]. Creatine kinase and troponin elevations in the blood are indicative of myocardial injury in patients. However, the elevation of creatine kinase and troponin after microinfarction can be undetected due to their dilution in the large sinus blood flow. A large meta-analysis of 23, 230 patients with stable or unstable angina undergoing PCI with follow-up for 6-34 months compared with the data from healthy volunteers showed a close relationship between creatine kinase - MB concentration and mortality rate, even at a minor increase of creatine kinase - MB 1–3x conferring a relative risk of death of 1.5 (95%) [17].

Non-invasive imaging

Ischemic heart disease can be detected directly on Positron Emission Tomography (PET) and Single-Photon Emission Computed Tomography (SPECT), MRI, Computed Tomography (CT), and indirectly on ECG, cardiac injury biomarkers, ventriculography, and echocardiography. PET, SPECT, CT and echocardiography have been the clinical modalities for assessing myocardial perfusion and viability, while intravascular imaging methods, such as Optical Coherence Tomography (OCT) and Intravascular Ultrasound (IVUS),

characterize plaque composition (large necrotic cores, high plaque volume, thin-capped fibroatheroma) [18-20]. Echocardiography is the most commonly used clinical method for quantification of global and regional LV function in patients with ischemic heart disease [21]. Investigators also used 2D speckle-tracking images to measure regional strain and strain rate [22] as well as LV remodeling [23] and reverse remodeling [24].

The variability of patient populations, micro-emboli volume/size, territory of feeding vessels and cardiac motion are major limitations in visualizing and quantifying microinfarct on MRI or drawing sound conclusions on the deleterious effects of micro-emboli. Thus, investigators found that preclinical animal models are suitable for resolving the above complexities of myocardial microinfarction [14,25-28].

Coronary microemboli on doppler

Porto, et al. [29-31] were the first to count coronary micro-emboli in real-time during PCI using High Intensity Transient Signals (HITS) derived from Doppler guide wire. The gold standard method of detecting the passage of emboli is the audible detection of the sudden "chirp" or "moan" produced by emboli as well as the visual detection of the time-frequency representation (spectrogram) generated on the Doppler screen. This method is based on calculating the energy from the spectrogram and applying constant thresholds to pick up the emboli. Clinical and preclinical studies shed light on the complex relationship between coronary interventions and myocardial microinfarct. Many studies linked coronary micro-emboli myocardial contractile dysfunction, malignant arrhythmias, perfusion deficits and coronary reserve impairment [5,9,29,30]. To the best of our knowledge, the detection of circulating coronary micro-emboli, using MRI, has not been performed and very challenging at the present time.

Myocardial microinfarct on MRI

Myocardial microinfarct are very small infarcts resulted from obstruction of coronary capillaries, arterioles, or small arteries. Thus, the small average size highlights the challenges in designing imaging methods for detecting microinfarct. Given a mean diameter of <1 mm_3, the size of most microinfarct is below the lower limit of spatial resolution (approximately 1 mm^3) for 1.5T and 3.0T MRI scanners used in clinical practice. Therefore, increased spatial resolution is needed for MRI to be able to detect microinfarct and differentiate them from other lesions. Increasing signal to noise ratio, using high field strengths (7.0T), might improve the contrast between microinfarct and viable tissue and thus aid visual detection.

Microinfarct are visible as hyper intense speckles (salt and pepper) on delayed contrast enhanced MR images (DE-MRI). Kwong, et al. [32] reported that even small infarct (1.4% of LV mass) identified on DE-MRI portended a > sevenfold increased risk for major adverse cardiac events. Bodi, et al. [24] found that assessment of infarct and micro vascular obstruction zone within the infarct on MRI soon after STEMI enabled the prediction of reverse remodeling.

Myocardial viability

Dynamic and delayed contrast enhanced MRI has used for demonstration of the success of revascularization after PCI. Regions with still impaired blood flow appear hypo enhanced (micro vascular obstruction zone), while infarcted regions appear hyper enhanced. In these cases, remote myocardium is moderately enhanced on dynamic MR imaging. This technique is based on measuring the delivery of MR contrast media to the myocardium during and after the first pass following a bolus injection using T1-weighted imaging sequences. Inversion recovery viability techniques, such as gradient echo and modified Look-Locker were used for visualization and quantification of myocardial infarct and micro vascular obstruction zone.

In an experimental MRI study, investigators found a positive correlation between micro-emboli volumes and myocardial infarct sizes [33]. MRI also demonstrated a large variation in the size of myocardial infarct after PCI (0.7-12.2 g or 0.4-6.0% LV) in patients [15]. In some cases microinfarct co-exist with other pathologies, such as revascularized grossly visible Acute Myocardial Infarction (AMI), where patchy microinfarct present in the peri-infarct zone [34,35]. Investigators reported multiple micro-embolic border zone in the brain, which was associated with endomyocardial fibrosis in a patient with idiopathic hypereosinophia using CT and pathological examination. Neuropathological examination revealed multiple arteriolar fibrinocruoric thrombi.

From a clinical perspective, patchy microinfarct in the peri-infarct zone is of pivotal importance for the prognosis and recovery of LV function and arrhythmia [34,35]. An electrophysiological study implicated the heterogeneity of depolarization and dispersion of repolarization to microinfarct within the peri-infarct zone and concluded that microinfarct at the peri-infarct zone is a key substrate in arrhythmia-related to sudden cardiac death [36]. Two studies confirmed that a large peri-infarct zone is associated with increased risk of mortality or major adverse events [37,38].

In a swine model, delivery of micro-emboli also caused arrhythmia and 25% mortality rate within the first 24 hrs [39] and this mortality rate is comparable to that observed in 90 min LAD occlusion/revascularization animals [40]. Experimental DE-MRI study also demonstrated the patchy myocardial enhancement 6 hrs after embolization [33,41,42]. Breuckmann, et al. [41] indicated that a threshold of 5% was necessary for visualization of microinfarct on DE-MRI. Furthermore, investigators reported that only visualized microinfarct on DE-MRI cause LV dysfunction in patients [43] (Figure 1). An MRI study showed that both visible and invisible microinfarct resulted in LV dysfunction [44] because this imaging modality underestimates microinfarct size compared to microscopy. In a recent proof-of-concept study, we demonstrated that mildly injured myocardium subjected to 40 min LAD occlusion then micro embolization did not manifest greater susceptibility to infarction compared with solely embolized non-ischemic myocardium and 40 min LAD occlusion groups [14] (Figure 2).

Breuckmann, et al. [41] reported that T2-weighted imaging was limited in detecting edematous area at risk 8 hrs after embolization. They attributed this limitation to the small difference (10%) in water content between embolized and remote myocardium [28]. More recently, T2-MRI for measurement of area at risk, based on the formation of interstitial edema, has been seriously criticized and disputed [45]. In a recent publication in patients and animals, Kim, et al. [46] indicated that T2-weighted MRI did not measure salvageable myocardium, but true infarct.

The equilibrium state of distribution of MRI contrast media in myocardium is used for evaluating myocardial viability based on the measurement of extracellular volumes. The distribution of MRI contrast media in normal myocardium is in the intravascular and interstitial spaces, while in infarcted myocardium, the myocytes lose their cellular integrity to become a part of the extracellular space, thus providing larger distribution volume compared with

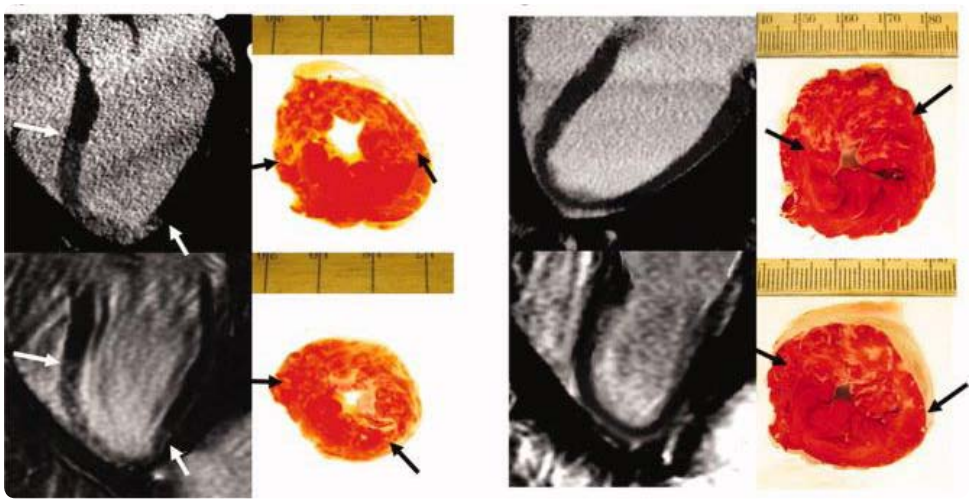

Figure 1: The variability in visualizing myocardial microinfarct on long-axis DE-MDCT (top left) and DE-MRI (bottom left) images in two animals after administration of 32 mm^3 (left block) and 16mm^3 of 40-120 μm micro-emboli (right block). DE-MDCT and DE-MRI long-axis view images showed speckled microinfarct along the inter-septal LV wall (left, white arrows) after administration of 32 mm^3 micro-emboli, but not 16 mm^3 micro-emboli. Unlike MDCT and MRI, TTC-stained sections illustrated microinfarct after administration of both micro-emboli volumes (black arrows).

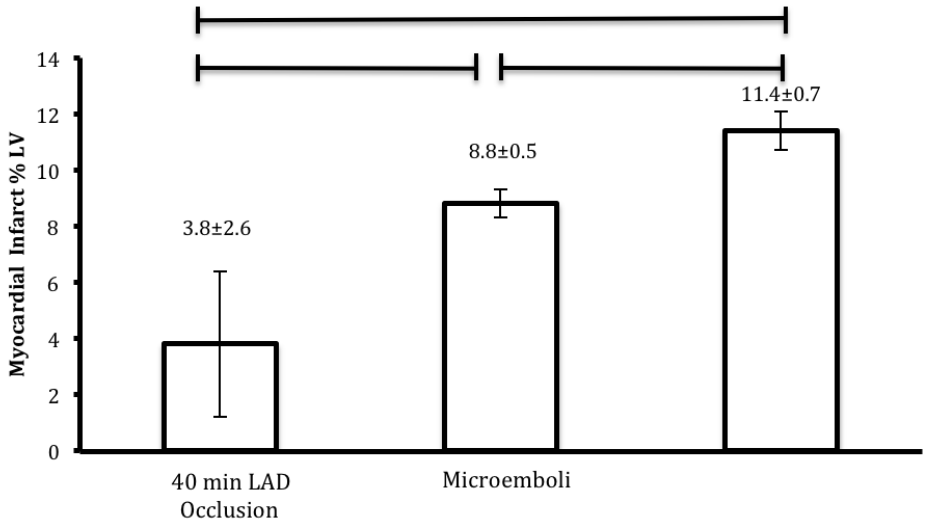

Figure 2: Bars show the incremental increase in myocardial infarct sizes in animals subjected to 40 min LAD occlusion/revascularization, coronary micro embolization by 32 mm3 micro-emboli or the combination of both insults.

normal myocardium. The technique was first used in detecting small myocardial damage in rats subjected to 20min LAD coronary artery occlusion/revascularization. Investigators found clear difference in fractional distribution volume between normal myocardium (18%) and patchy infarcted myocardium (32%). Ischemic myocardium demonstrated dispersed focal cellular necrosis involving 18% of the cells per field under microscope [47].

The recent advancements of high field MR scanners and sequences for mapping T1 relaxation time allow scientists and clinicians to explore minor pathologic changes in myocardium. Investigators showed that T1 mapping sequences had the potential to demonstrate regional T1 changes associated with edema and diffused fibrosis [48-54]. T1-and T2-mapping images showed increases in native T1- and T2-relaxation times and a decrease in T1-relaxation time in MI post-contrast media injection too [54,55]. Native T1-mapping drew more attentions of clinicians, as it did not require contrast media and was accessible in the context of renal impairment or contrast allergies [55,56].

LV function

Accurate assessment of LV function is essential for the diagnosis, therapeutic management and prognosis. Cine MRI offers great advantage over echocardiography by providing a set of contiguous short-axis MRI LV and RV slices from the base to the apex, and long-axis views. The ECG-triggered cine MRI sequences provide data on cardiac mass, volumes, and 3-D strains (radial, circumferential and longitudinal) after microembolization [27,33,57-59]. Such data can be combined with myocardial perfusion, viability and coronary flow. Carlsson, et al. [57] demonstrated the deleterious effects of relatively large micro-emboli (100-300 μm diameter, 70 mm^3) on regional LV radial strain in swine model. Cine MRI showed the changes in LV volumes and ejection fraction at 1 hour and 1 week after microembolization compared to baseline, which might be attributed

to the persistent decline in the radial strain of the embolized region (Figure 3). In another study, a decline in ejection fraction from 49 ± 1% at baseline to 29% ± 1 at 1 hr (P = 0.02) and 36% ± 1 at 1 week after delivery of 7500 micro-emboli of 100-300 μm diameter was documented [58]. There was poor correlation between the ejection fraction and microinfarct size (r = 0.20) at 1 hr or at 1 week (r = 0.54). Similarly, the correlation was poor between the ejection fraction and the extent of perfusion deficit at 1 hr (r = 0.27) or 1 week (r = 0.39) [59]. Our findings of persistent declines in regional and global functions at 1 week using relatively large emboli (100-300 μm in diameter) are in line with findings in sheep using 90 μm emboli [60]. However, heterogeneity among studies exists. For example, a study in dogs showed that LV dysfunction occurred within hours after delivering of small embolic agent (42 μm) followed by a complete recovery of function within 5-6 days [25].

We also compared the effects of two micro-emboli volumes (16 and 32 mm^3) on regional and global LV function and found that the effect of 32 mm^3 micro-emboli on radial stain was broader (involved at least 4 segments in basal, mid and apical MRI slices) than animals that received 16 mm^3 micro-emboli. At the global level, micro-emboli caused acute increases in LV diastolic and systolic volumes (Figure 4). Furthermore, LV ejection fraction was significantly lower in animals that received 32 mm^3 than 16 mm^3 micro-emboli [44]. Serial MRI studies showed that coronary microembolization led to LV remodeling and persistent decline in systolic wall thickening [39,58,61,62].

In another swine study, we explored the potential of cine MRI for quantifying the effects of defined micro-emboli volumes and sizes on LV function in preexisting 3 days old AMI [44]. Animals subjected to LAD occlusion/microembolization/revascularization showed greater LV wall thinning, decrease in ejection fraction and increase in end-systolic volume than controls and animals subjected to LAD occlusion/revascularization (Figure 5). Quantitative analysis showed a total of 576 segments with systolic wall thickening were graded as normal with a thickening of more than 30% in 192 segments of control, 112 segments of animals subjected to LAD occlusion/revascularization and 64 segments of animals subjected to microembolization in preexisting AMI; hypokinetic, with 10%-

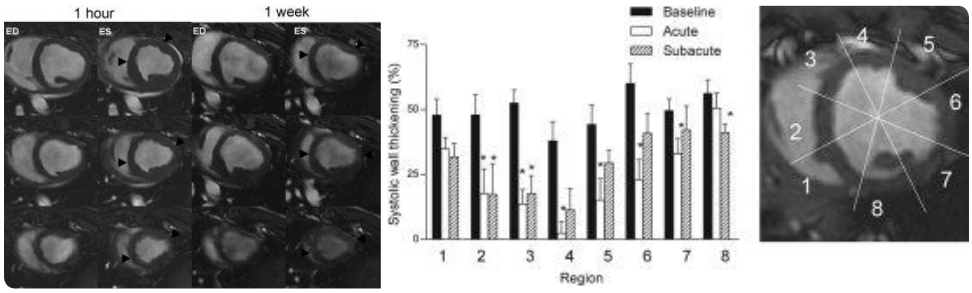

Figure 3: Left block: three slices cine MRI at 1 h (left) and 1 week (right) after micro embolization acquired at end diastole and end systole. Decreased function is seen in the anteroseptal wall (black arrowheads). Right block: Radial strain (systolic wall thickening) is shown in eight segments at baseline, 1 h, and 1 week. The area of micro embolization is located between segments 2 and 5 and shows dysfunction. The MR image (right) shows the location of the regions used for analysis of wall thickening. *P < 0.05 compared to baseline.

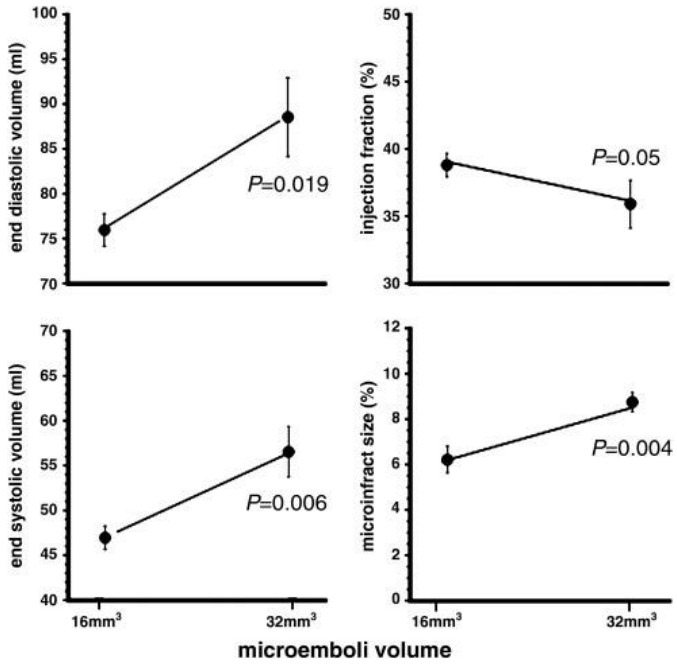

Figure 4: The effects of two different micro-emboli volumes are shown on LV end diastolic volume (top left), end systolic volume (bottom left), ejection fraction (top right) measured on cine MRI and speckled enhanced microinfarct size (bottom right) on DE-MRI. All the parameters show significant difference related to the micro-emboli volumes.

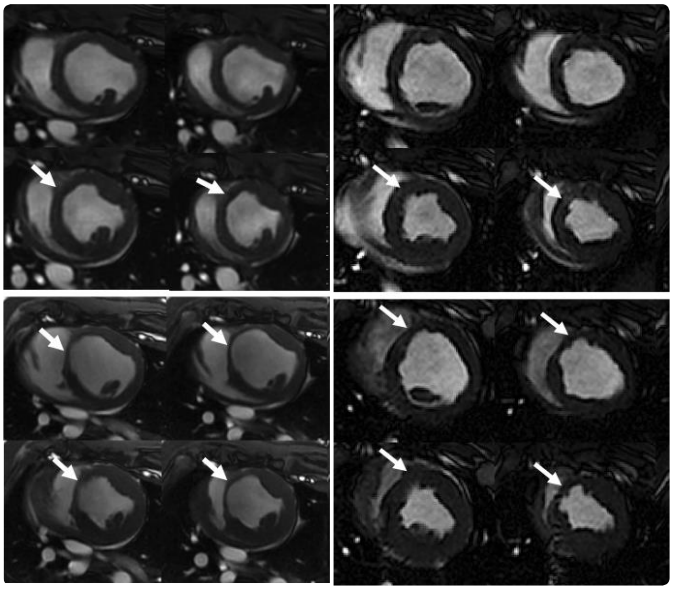

Figure 5: Cine MRI. Left: Multislice diastolic (top row) and systolic (bottom row) cine MR images acquired at 3 days (top block) and 5 weeks (bottom block) from an animal subjected to 90 min LAD occlusion/revascularization. White arrows point to the site of infarction and show wall thinning at 5 weeks. Right: Multislice diastolic (top row) and systolic (bottom row) cine MR images acquired at 3 days (top block) and 5 weeks (bottom block) in an animal subjected to 90 min LAD occlusion/microembolization/revascularization. At 5 weeks, the site of infarction (arrows) show greater wall thinning compared with 90 min LAD occlusion/revascularization.

29% systolic wall thickening in 48 segments in LAD occlusion/revascularization as well as in animals subjected to micro-emboli in preexisting AMI groups, akinetic with 0%–9% systolic wall thickening in 32 segments in LAD occlusion/revascularization as well as in animals subjected to micro-emboli in preexisting AMI. Dyskinesis and paradoxical systolic-wall thinning were observed only 48 segments of animals subjected to LAD occlusion/microembolization/revascularization. Circumferential and longitudinal wall strains were also depressed after coronary microembolization [59]. Suhail, et al. [59] found that cine and tagged MRI sequences were useful for measuring left/right ventricles longitudinal and circumferential strains in patchy microinfarct and large infarct, respectively. HARP and plane metric software are used to quantify circumferential and longitudinal strains in microembolized infarct. Investigators observed that coronary micro-emboli caused greater impairment in LV circumferential strain and dyssynchrony than 90 min LAD occlusion/revascularization animals despite the significant differences in infarct sizes. Micro-emboli also caused a significant decrease in peak systolic strain rate of remote myocardium and LV dyssynchrony. Compensatory increase in longitudinal strain of RV free wall was also observed in response to micro-emboli delivered in the LAD and LAD occlusion/revascularization animals. This study concluded that 1) coronary micro-emboli with or without AMI core caused complex myocardial injury and ventricular dysfunction that were not replicable in solely AMI and 2) there was a disproportion in the declines of circumferential strain, dyssynchrony, and infarct size of animals subjected to microembolization and AMI. A clinical study showed that longitudinal strains measured on cine MRI correlated well with infarct sizes [63], while Galiuto, et al. [64] indicated that the improvement in longitudinal strain was an index of myocardial viability, associated with global LV improvement and possibly reverse remodeling, which is an important predictor of favorable long-term outcomes. Future studies are needed to determine the potential roles of inflammation and oxidative stress in promoting cardiac dysfunction using PET/MRI techniques.

Myocardial perfusion

The severity and extent of myocardial ischemia is a key to decision-making for revascularization. With commencing myocardial ischemia, a cascade of cellular, functional and electrocardiographic events ensues. Thallium-201 scintigraphy studies demonstrated that coronary stenosis causes perfusion deficits [65,66]. Investigators also observed a mismatch between LV dysfunction and epicardial coronary blood flow after revascularization [67]. First pass MRI also detected myocardial perfusion deficits in patients after PCI [30,68].

In general, microembolized myocardium with and without pre-existing infarct is defined as hypo enhanced zone on first pass MRI**.** Unlike DE-MRI, perfusion imaging has the potential to detect early effect of micro-emboli (as early as 1 hr) on myocardium perfusion (Figure 6). Maximum upslope, maximum SI and time to the peak obtained from first pass MRI perfusion are the best indices to estimate regional perfusion deficits [33,44,57,69]. Quantitative analysis of perfusion parameters revealed in these studies that the maximum signal intensity and time to peak were lower and longer, respectively, in both acute and scar microinfarct compared with remote myocardium. Selvanayagam, et al. [70] used first pass perfusion and DE-MRI to demonstrate perfusion deficits and new microinfarct 24 hrs after PCI. Choi, et al. [43] found an association between perfusion deficits and discrete AMI in patients after PCI.

In an experimental study, Mohlenkamp, et al. [71] investigated the changes in coronary microcirculation (intra myocardial microvascular blood volume, perfusion, transit time and pattern of microvascular injury) in response to different sizes of micro-emboli. They observed that 100μm microspheres resulted in patchy plugging, while 10μm microspheres induced contiguous hemorrhagic myocardial injury. Skyschally, et al. [68] demonstrated a lack of changes in baseline coronary blood flow after stepwise repeated injections of microsphere (42 μm diameter) using Doppler flow meter. In contrast, Ma, et al. [61] observed in swine the reductions in coronary flow reserve and LV ejection fraction 6 hours after emboli injection (42 μm, 120,000) into LAD. The animals showed complete recoveries of flow reserve

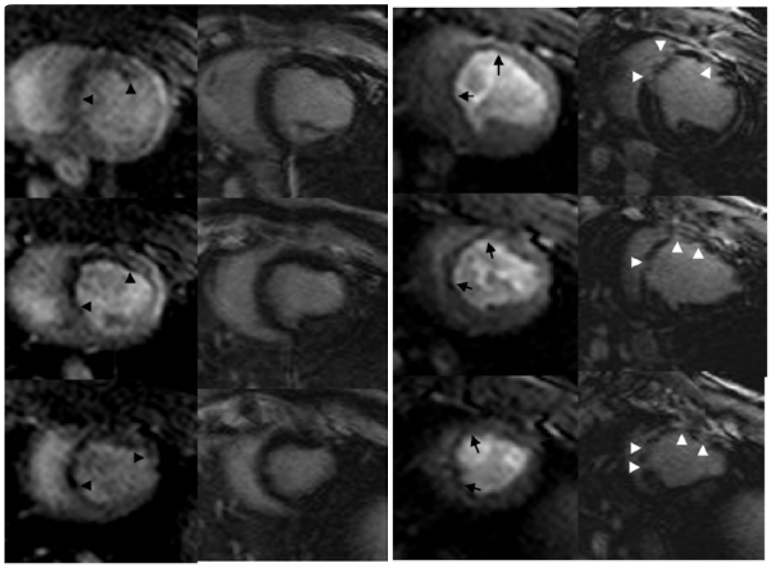

Figure 6: Multislice first pass perfusion MR images acquired 1 hr (left, left block) and 1 week (left, right block) after LAD embolization in swine show the persistent perfusion deficit in embolized myocardium. DE-MR images acquired 1hr after embolization failed to demonstrate myocardial microinfarct. On the contrary, DE-MRI provided evidence of microinfarct at 1 week.

and LV ejection fraction, but LV dilation, 1 week later. Bai, et al. [72] also reported a persistent LV dysfunction and progressive remodeling in swine model 28 days after repeated microsphere injection.

Microinfarct on computed tomography

With the improvements in spatial and temporal resolutions and reduction in radiation exposure, Multi-Detector Computed Tomography (MDCT) has evolved into major clinical noninvasive coronary artery imaging modality. MDCT has been used for visualizing microinfarct and detecting LV dysfunction in embolized myocardium in beating swine heart model [39,73-75].

CT contrast media have extracellular distribution, thus theoretically, their kinetics is parallels to those of gadolinium chelates. On the basis of this hypothesis Jablonowski, et al. [75] assessed myocardial extracellular volumes in normal myocardium, contiguous infarct and patchy microinfarct. They found that the fractional distribution volume was 24% in viable myocardium, 36% in microinfarct after delivery of 16 mm^3 micro-emboli, 41% in microinfarct after delivery of 32 mm^3, 55% in large infarct after 90 min LAD occlusion/revascularization and 56% after 90 min LAD occlusion/revascularization with delivery of 32 mm^3 micro-emboli. The microscopic measurements confirmed MDCT data. Regression analysis revealed excellent correlation between regional myocardial extracellular volume on MDCT and microscopy (r^2 = 0.92). On micro-CT, Malyar, et al. [76] identified in vitro the patchy pattern of perfusion in micro embolized myocardium and attributed it to a random distribution and clustering of micro-emboli in micro vessels. However, computed tomography has limitations, such as poor temporal resolution, artifacts, radiation exposure and contrast-induced nephropathy.

Microinfarct on microscopy

Micro infarct appears to share the histopathologic structure and progression of macroscopic infarcts. Gu, et al. [10] observed under light and electron microscope that delivery of auto micro thrombotic particles into the coronary arteries induced micro thrombosis, damage of vascular endothelium, and microinfarct. Other investigators showed that monocytes/macrophages dominated the cellular infiltrates for the first 2 weeks after MI and participated in wound healing [77,78]. Frangogiannis, et al. [79] classified the healing process of myocardial infarct into 3 distinct but overlapping phases; the inflammatory, proliferative and maturation, while Nahrendorf, et al. [80] summarized the roles of monocytes/macrophages in infarct healing, including 1) release inflammatory mediators; 2) release proteases; 3) phagocytose apoptotic and necrotic myocytes and neutrophils and other debris; 4) promote angiogenesis; 5) transport reparative enzymes and prosurvival factors; and 6) stimulate collagen synthesis and deposition by myofibroblasts. It has been shown that multiple injections of microspheres induce macro-infarct [72]. Necrotic myocyteswere generally found in the form of large or small islands depending on the size of obstructed micro vessels. (Figure 7) shows the patchy microinfarct and infiltration of inflammatory cells in infarcted myocardium 3 days after microembolization, confirming a previous study [44]. Myocardial inflammation usually starts as early as 30 minutes at the infarct borders to clear cellular debris [81] and the number of macrophages peaks on the third day [82,83]. Bai, et al. [72] also observed an early increased inflammatory activity followed by persistent pro-inflammatory cytokines protein expression and collagen deposition. The use of iron particles, as MR contrast medium, might be helpful in noninvasively identifying and quantifying temporal changes in myocardial inflammation [84,85]. Monitoring macrophages/monocytes infiltration might be useful for predicting clinical outcomes and monitoring the beneficial effects of immune-modeling therapy [86].

Aged microinfarct cannot be differentiated from acute micro infarct based on signal intensity, but microscopically based on the lack of inflammatory cells and interstitial edema [14,27,87]. At 5 weeks, macro-infarct showed scar tissue and remodeled blood vessels with a thick wall and small lumen, but macro-infarct superimposed with micro-emboli injection still have obstructed micro vessels (Figure 8). Furthermore, at this time micro-emboli start to migrate to the peri-vascular space and by 8 weeks they are settled in the

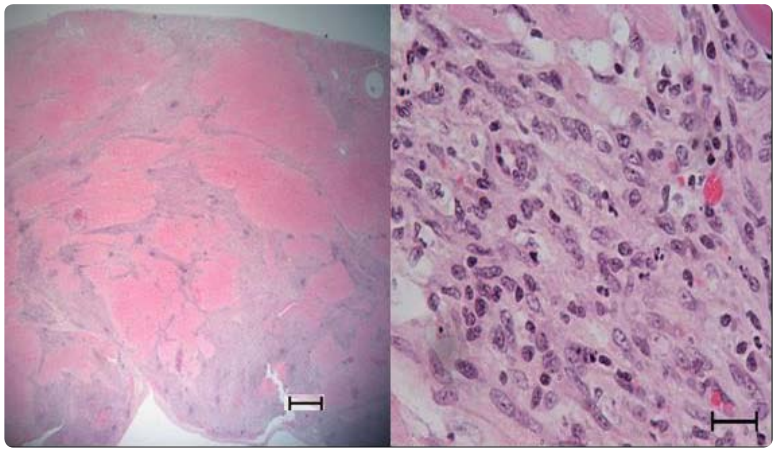

Figure 7: Microscopic sections show the patchy microinfarct and infiltration of inflammatory cells in infarcted myocardium 3 days after coronary microembolization (10X and 100X).

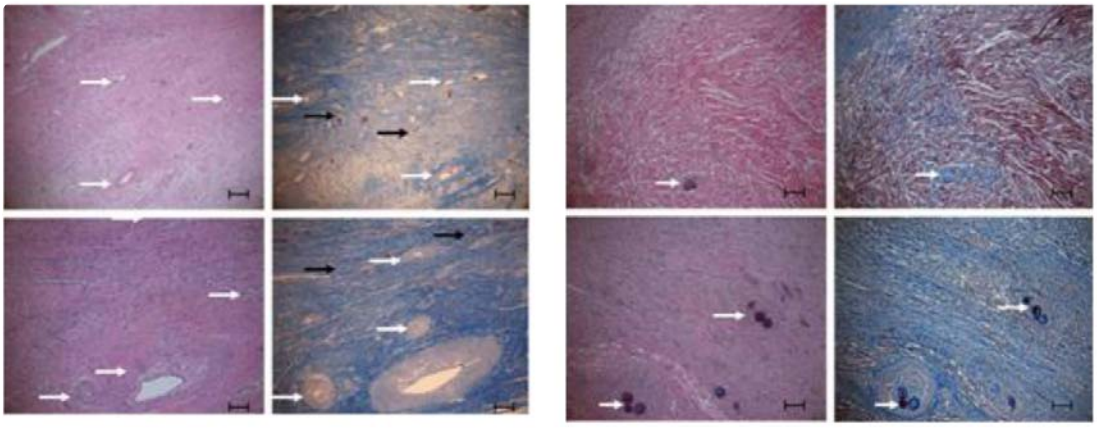

Figure 8: Microscopic sections show the differences at the cellular and vascular levels between 90 min LAD occlusion/ revascularization at 5 weeks (left block) and 90 min LAD occlusion/microembolization/revascularization at 5 weeks (right block) animals using H&E and Masson trichrome stain. The former animal showed remodeled blood vessels with a thick wall and small lumen (white arrows) and new patent vessels (black arrows), but no evidence of obstructed vessels. The later animal showed complete obstruction of microvessels by fibrotic tissue, debris and inflammatory cells.

peri-vascular space (Figure 9). Interestingly, interstitial edema was evident at 5 weeks in remote myocardium of animals subjected to macro-infarct and coronary microembolization, but not of animals subjected to only macro-infarct (Figure 10). Furthermore at 5 weeks, animals subjected to macro-infarct and microembolization showed less infarct resorption (slow healing) and LV dilation than animals subjected to macro-infarct only (Figure 11) [27]. These findings prove the conjecture by Kloner, et al. [88] and Wu, et al. [89] that microvascular obstruction delayed/inhibited optimal infarct healing by slowing the delivery of inflammatory cells and nutrients. It has been shown that slow infarct healing can lead to LV remodeling, infarct rupture and death [90].

A clinical MRI investigation showed that the resorption of large infarct was faster than small infarct [91]. On the contrary in swine, MRI and histologic study demonstrated that the resorption of microinfarct was faster than large infarct [14]. At 5 weeks, the resorption of macro-infarct was substantially greater than macro-infarct with microinfarct (60% and 25%, respectively) [14,92]. Choi, et al. [93] and Inkangisorn, et al. [94] found in patients a decline in infarct sizes of 27% and 31%, respectively, 2 months after infarction.

In a recent preclinical study, Grutzendler, et al. [95] proved that micro-emboli could be cleared from microvessels by angiophagy, in which emboli were engulfed by the endothelium and they translocated through the microvascular wall. The engulfment of emboli by the endothelial membrane projections leads to reestablishment of blood flow, vessel sparing and salvaged ischemic tissues. The molecular control of the extravasation mechanism involves mechano transduction, vascular plasticity, cytoskeletal dynamics and remodeling of endothelial junctions [96]. We also documented in large animal model the migration of microemboli from the intravascular compartment to the interstitium of myocardium using serial histologic studies (Figure 9). In previous preclinical studies we found that LV mass was significantly larger in animals subjected to coronary occlusion/ delivery of micro-emboli/revascularization for over 5 weeks than controls and animals subjected to occlusion/ revascularization (Figure 11) [14,87].

Treatment of myocardial microinfarct

Chen, et al. [97] recently found that glucocorticoid therapy improved LV function after coronary embolization through the suppression of transforming growth factor-beta 1 (TGF-β1)/

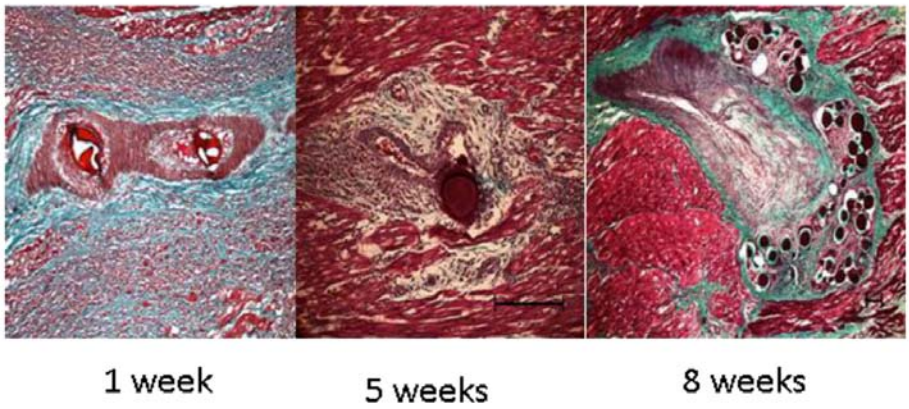

Figure 9: Myocardial sections stained with Mass on trichrome stain to demonstrate scar tissue and intact coronary blood vessels (X200). The 3 sections show the migration of micro-emboli from the intravascular space into the peri-vascular space as a function of time. Up to one week the micro-emboli occupy the intravascular space. At 5 weeks the micro-emboli start to migrate into the peri-vascular space and 8 weeks almost all micro-emboli are located in the peri-vascular space.

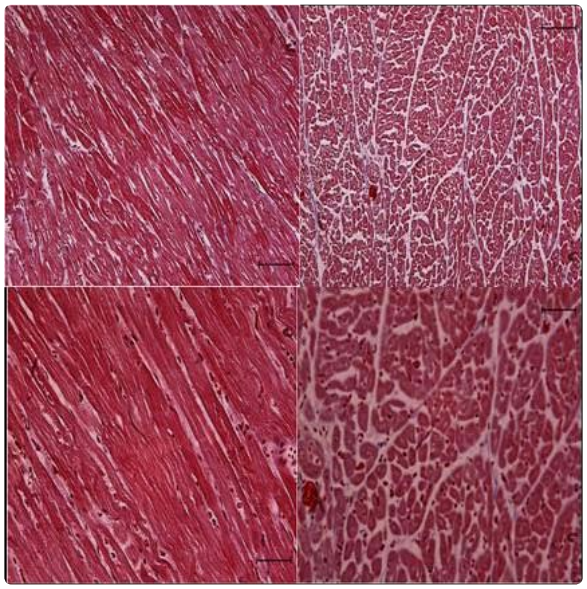

Figure 10: Microscopic sections show remote myocardium in animals subjected to 90 min LAD occlusion/revascularization (left) and 90 min LAD occlusion/microembolization/revascularization (right). The interstitial edema is evident only in LAD occlusion/microembolization/revascularization 5 weeks after the interventions (40X and 100X).

Smad3 and connective tissue growth factor. It also attenuated LV remodeling caused by microinfarct [62]. Jin, et al. [98] found a less decline in regional wall motion in the embolized area in animals treated with glucocorticoid (methyl prednisone, as anti-inflammatory therapy) than control animals at 6 hrs after coronary micro embolization. Methyl prednisone administration ameliorated myocardial dysfunction (88.6 ± 7.6%) compared with control group (47.7 ± 4.7%; $P< 0.001$) at 6 hrs after embolization. The systolic wall-thickening index was at the baseline, 96.3 ± 8.2%. The LV ejection fraction decreased from 49.9 ± 3.5% at baseline to 34.6 ± 3.7% at 6 hours ($P < 0.001$) in the control group, which was significantly less in treated group from 47.1 ± 3.8% to 42.5 ± 3.9%. Other found that statins, anti platelet agents, and coronary vasodilators could protect the myocardium from micro-emboli when administered prior to PCI. Distal protection devices may retrieve atherothrombotic debris, but their effects are controversial.

Experimental studies revealed that the phosphatase and tensin homolog deleted on chromosome Ten (PTEN) were proteins regulating inflammation and apoptosis. Apoptotic bodies were evident in microembolized and remote myocardium using cleaved caspase 3 stain [33,99]. This protein is highly expressed in reperfused AMI and it enhances inflammation after embolization [100]. Investigators found that inhibition of PTEN improved myocardial function by attenuating myocardial apoptosis [26].

In conclusion, clinical and preclinical studies shed light on the complex relationship between coronary interventions and myocardial microinfarct. MRI has been proven to reliably estimate regional perfusion and LV function of micro embolized myocardium. The visibility of microinfarct on DE-MRI, however, is limited and dependents on technical issues, such as optimization of the inversion time, elimination of motion artifacts and MR contrast media relaxativity/kinetics as well as biological issues, such as micro-emboli volume, age of microinfarct and collateral circulation. MRI has not been used for counting circulating micro-emboli during coronary

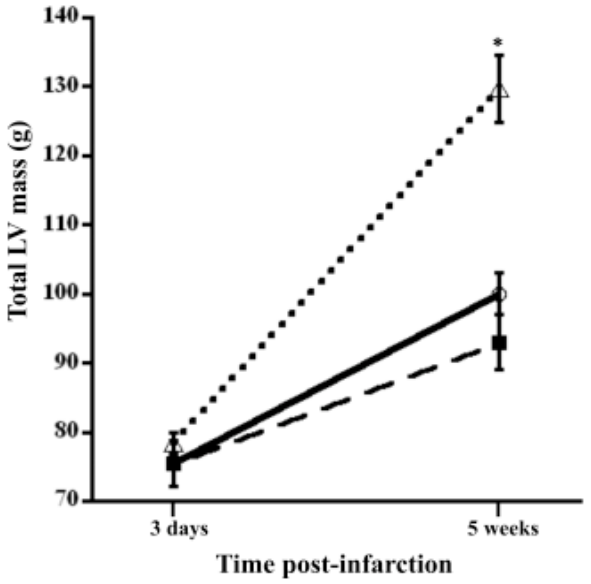

Figure 11: A plot showing the differential increase in LV masses over the course of 5 weeks in control (dashed line), 90min LAD occlusion/ revascularization (continuous line) and 90 min LAD occlusion/ microembolization/revascularization animals (dotted line).
*P < 0.001 compared with the other two groups.

interventions. Microscopic examination of biopsyis for confirming the presence of microvascular obstruction, caused by micro-emboli, but obtaining biopsy is not recommended in routine clinic. At this time, there is no known drugs/device that has demonstrated conclusively myocardial protection. For advancement of clinical care it is of paramount importance to develop innovative techniques/ drugs for detecting, capturing micro-emboli and treating myocardial infarction.

REFERENCES

1. Moody DM, Bell MA, Challa VR, Johnston WE, Prough DS. Brain microemboli during cardiac surgery or aortography. Annals of Neurology, 1990; 28: 477-486.
2. Rezkalla SH, Kloner RA. No-reflow phenomenon. Circulation. 2002; 105: 656-662.
3. DeFrances CJ, Lucas CA, Buie VC, Golosinskiy A. 2006 National Hospital Discharge Survey, 2008, U.S. Department of Health and Human Services. Centers for Disease Control and Prevention National Center for Health Statistics Hyattsville, MD.
4. Cuculi F, Lim CC, Banning AP. Periprocedural myocardial injury during elective percutaneous coronary intervention: is it important and how can it be prevented? Heart. 2010; 96: 736-740.
5. Topol EJ, Yadav JS. Recognition of the importance of embolization in atherosclerotic vascular disease. Circulation. 2000: 101: 570-580.
6. Kotani J, Mintz GS, Pregowski J, Kalinczuk L, Pichard AD, Satler LF, et al. Volumetric intravascular ultrasound evidence that distal embolization during acute infarct intervention contributes to inadequate myocardial perfusion grade. American Journal of Cardiology. 2003; 92: 728-732.
7. Henriques JP, Zijlstra F, Ottervanger JP, De Boer MJ, Van't Hof AW, Hoorntje JC, et al. Incidence and clinical significance of distal embolization during primary angioplasty for acute myocardial infarction. Eurean Heart Journal, 2002; 23: 1112-1117.
8. Nallamothu BK, Bates ER. Periprocedural myocardial infarction and mortality: causality versus association. Journal of American College of Cardiology. 2003; 42: 1412-1414.
9. Schwartz RS, Burke A, Farb A, Kaye D, Lesser JR, Henry TD, et al. Microemboli and microvascular obstruction in acute coronary thrombosis and sudden coronary death: relation to epicardial plaque histopathology. Journal of American College of Cardiology. 2009; 54: 2167-2173.
10. Gu Y, Bai Y, Wu J, Hu L, Gao B. Establishment and characterization of an experimental model of coronary thrombotic microembolism in rats. American Journal of Pathology. 2010; 177: 1122-1130.
11. Serruys PW, Morice MC, Kappetein AP, Colombo A, Holmes DR, Mack MJ, et al. Percutaneous coronary intervention versus coronary-artery bypass grafting for severe coronary artery disease. New England Journal of Medicine. 2009; 360: 961-972.
12. Troncoso JC, Zonderman AB, Resnick SM, Crain B, Pletnikova O, O'Brien RJ. Effect of infarcts on dementia in the Baltimore longitudinal study of aging. Annals of Neurology. 2008; 64: 168-176.
13. Prizel KR, Hutchins GM, Bulkley BH. Coronary Artery Embolism and Myocardial InfarctionA Clinicopathologic Study of 55 Patients. Annals of Internal Medicine. 1978; 88: 155-161.
14. Do L, Wilson MW, Krug R, Hetts SW, Saeed M. MRI monitoring of function, perfusion and viability in microembolized moderately ischemic myocardium. The International Journal of Cardiovascular Imaging. 2015; 31: 1179-1190.
15. Ricciardi MJ, Wu E, Davidson CJ, Choi KM, Klocke FJ, Bonow RO, et al. Visualization of discrete microinfarction after percutaneous coronary intervention associated with mild creatine kinase-MB elevation. Circulation. 2001; 103: 2780-2783.
16. Selvanayagam JB, Porto I, Channon K, Petersen SE, Francis JM, Neubauer S, et al. Troponin elevation after percutaneous coronary intervention directly represents the extent of irreversible myocardial injury: insights from cardiovascular magnetic resonance imaging. Circulation. 2005; 111: 1027-1032.
17. Ioannidis JP, Karvouni E, Katritsis DG. Mortality risk conferred by small elevations of creatine kinase-MB isoenzyme after percutaneous coronary intervention. Journal of American College of Cardiology. 2003; 42: 1406-1411.
18. Bose D, von Birgelen C, Zhou XY, Schmermund A, Philipp S, Sack S, et al. Impact of atherosclerotic plaque composition on coronary microembolization during percutaneous coronary interventions. Basic Research of Cardiology. 2008; 103: 587-597.
19. Hong YJ, Mintz GS, Kim SW, Lee SY, Okabe T, Pichard AD, et al. Impact of plaque composition on cardiac troponin elevation after percutaneous coronary intervention: an ultrasound analysis. JACC. Cardiovascular imaging. 2009; 2: 458-468.
20. Uetani T, Amano T, Ando H, Yokoi K, Arai K, Kato M, et al. The correlation between lipid volume in the target lesion, measured by integrated backscatter intravascular ultrasound, and post-procedural myocardial infarction in patients with elective stent implantation. European Heart Journal. 2008; 29: 1714-1720.
21. Lang, RM, Bierig M, Devereux RB, Flachskampf FA, Foster E, Pellikka PA, et al. Recommendations for Chamber Quantification: A Report from the American Society of Echocardiography's Guidelines and Standards Committee and the Chamber Quantification Writing Group, Developed in Conjunction with the European Association of Echocardiography, a Branch of the European Society of Cardiology. Journal of the American Society of Echocardiography. 2005; 18: 1440-1463.
22. Møller JE, Hillis GS, Oh JK, Reeder GS, Gersh BJ, Pellikka PA. Wall motion score index and ejection fraction for risk stratification after acute myocardial infarction. American Heart Journal. 2006; 151: 419-425.
23. Reisner SA, Lysyansky P, Agmon Y, Mutlak D, Lessick J, Friedman Z. Global longitudinal strain: a novel index of left ventricular systolic function. Journal of the American Society of Echocardiography. 2004; 17: 630-633.
24. Bodi V, Monmeneu JV, Ortiz-Perez JT, Lopez-Lereu MP, Bonanad C, Husser O, et al. Prediction of Reverse Remodeling at Cardiac MR Imaging Soon after First ST-Segment–Elevation Myocardial Infarction: Results of a Large Prospective Registry. Radiology. 2016; 278: 54-63.
25. Skyschally A, Haude M, Dorge H, Thielmann M, Duschin A, van de Sand A, et al. Glucocorticoid treatment prevents progressive myocardial dysfunction resulting from experimental coronary microembolization. Circulation. 2004; 109: 2337-2342.
26. Skyschally A, Gres P, Hoffmann S, Haude M, Erbel R, Schulz R, et al.

Bidirectional role of tumor necrosis factor-alpha in coronary microembolization: progressive contractile dysfunction versus delayed protection against infarction. Circulation research. 2007; 100: 140-146.

27. Bajwa HZ, Do L, Suhail M, Hetts SW, Wilson MW, Saeed M. MRI demonstrates a decrease in myocardial infarct healing and increase in compensatory ventricular hypertrophy following mechanical microvascular obstruction. Journal of Magnetic Resonance Imaging. 2014; 40: 906-914.

28. Heusch P, Nensa F, Heusch G. Is MRI Really the Gold Standard for the Quantification of Salvage From Myocardial Infarction? Circulation Research. 2015; 117: 222-224.

29. Porto I, Selvanayagam JB, Van Gaal WJ, Prati F, Cheng A, Channon K, et al. Plaque volume and occurrence and location of periprocedural myocardial necrosis after percutaneous coronary intervention: insights from delayed-enhancement magnetic resonance imaging, thrombolysis in myocardial infarction myocardial perfusion grade analysis, and intravascular ultrasound. Circulation. 2006; 114: 662-669.

30. Bahrmann P, Werner GS, Heusch G, Markus Ferrari, Tudor C. Poerner, et al. Detection of coronary microembolization by Doppler ultrasound in patients with stable angina pectoris undergoing elective percutaneous coronary interventions. Circulation. 2007; 115: 600-608.

31. Porto I, Biasucci LM, De Maria GL, Leone AM, Niccoli G, Burzotta F, et al. Intracoronary microparticles and microvascular obstruction in patients with ST elevation myocardial infarction undergoing primary percutaneous intervention. European Heart Journal. 2012; 33: 2928-2938.

32. Kwong RY, Chan AK, Brown KA, Chan CW, Reynolds HG, Tsang S, et al. Impact of unrecognized myocardial scar detected by cardiac magnetic resonance imaging on event-free survival in patients presenting with signs or symptoms of coronary artery disease. Circulation. 2006; 113: 2733-2743.

33. Saeed M, Hetts SW, Do L, Wilson MW. MRI study on volume effects of coronary emboli on myocardial function, perfusion and viability. International Journal of Cardiology, 2013. 165: 93-99.

34. Yan AT, Shayne AJ, Brown KA, Gupta SN, Chan CW, Luu TM, et al. Characterization of the peri-infarct zone by contrast-enhanced cardiac magnetic resonance imaging is a powerful predictor of post-myocardial infarction mortality. Circulation. 2006; 114: 32-39.

35. O'Regan DP, Ahmed R, Neuwirth C, Tan Y, Durighel G, Hajnal JV, et al. Cardiac MRI of myocardial salvage at the peri-infarct border zones after primary coronary intervention. American Journal of Physiology. Heart and Circulatory Physiology. 2009; 297: H340-H346.

36. Crawford T, Cowger J, Desjardins B, Kim HM, Good E, Jongnarangsin K, et al. Determinants of Postinfarction Ventricular Tachycardia. Circulation: Arrhythmia and Electrophysiology. 2010; 3: 624-631.

37. Demirel F, Adiyaman A, Timmer JR, Dambrink JH, Kok M, Boeve WJ, et al. Myocardial scar characteristics based on cardiac magnetic resonance imaging is associated with ventricular tachyarrhythmia in patients with ischemic cardiomyopathy. International Journal of Cardiology. 2014; 177: 392-399.

38. Kwon DH, Asamoto L, Popovic ZB, Kusunose K, Robinson M, Desai M, et al. Infarct characterization and quantification by delayed enhancement cardiac magnetic resonance imaging is a powerful independent and incremental predictor of mortality in patients with advanced ischemic cardiomyopathy. Circulation Cardiovascular Imaging. 2014; 7: 796-804.

39. Carlsson M, Saloner D, Martin AJ, Ursell PC, Saeed M. Heterogeneous microinfarcts caused by coronary microemboli: evaluation with multidetector CT and MR imaging in a swine model. Radiology. 2010; 254: 718-728.

40. Angeli FS, Shapiro M, Amabile N, Orcino G, Smith CS, Tacy T, et al. Left ventricular remodeling after myocardial infarction: characterization of a swine model on beta-blocker therapy. Compative Medicine. 2009; 59: 272-279.

41. Breuckmann F, Nassenstein K, Bucher C, Konietzka I, Kaiser G, Konorza T, et al. Systematic Analysis of Functional and Structural Changes After Coronary Microembolization: A Cardiac Magnetic Resonance Imaging Study. JACC: Cardiovascular Imaging. 2009; 2: 121-130.

42. Nassenstein K, Breuckmann F, Bucher C, Kaiser G, Konorza T, Schäfer L, et al. How much myocardial damage is necessary to enable detection of focal late gadolinium enhancement at cardiac MR imaging? Radiology. 2008; 249: 829-835.

43. Choi JW, Gibson CM, Murphy SA, Davidson CJ, Kim RJ, Ricciardi MJ. Myonecrosis following stent placement: association between impaired TIMI myocardial perfusion grade and MRI visualization of microinfarction. Catheter Cardiovascular Intervention. 2004; 61: 472-476.

44. Saeed M, Hetts SW, Do L, Wilson MW. Coronary microemboli effects in preexisting acute infarcts in a swine model: cardiac MR imaging indices, injury biomarkers, and histopathologic assessment. Radiology. 2013; 268: 98-108.

45. Fernández-Jiménez R, Fuster V, Ibanez B. Reply Myocardial Edema Should Be Stratified According to the State of Cardiomyocytes Within the Ischemic Region. Journal of the American College of Cardiology. 2015; 65: 2356-2357.

46. Kim HW, Van Assche L, Jennings RB, Wince WB, Jensen CJ, Rehwald WG, et al. Relationship of T2-Weighted MRI Myocardial Hyperintensity and the Ischemic Area-At-Risk. Circulation Research. 2015; 117: 254-265.

47. Arheden H, Saeed M, Higgins CB, Gao DW, Ursell PC, Bremerich J, et al. Reperfused rat myocardium subjected to various durations of ischemia: estimation of the distribution volume of contrast material with echo-planar MR imaging. Radiology. 2000; 215: 520-528.

48. Piechnik S, Ferreira V, Lewandowski A, Ntusi NA, Banerjee R, Holloway C, et al. Normal variation of magnetic resonance T1 relaxation times in the human population at 1.5 T using ShMOLLI. Journal of Cardiovascular Magnetic Resonance. 2013; 15: 13.

49. Fontana M, Banypersad SM, Treibel TA, Maestrini V, Sado DM, White SK, et al. Native T1 Mapping in Transthyretin Amyloidosis. JACC: Cardiovascular Imaging. 2014; 7: 157-165.

50. Puntmann VO, Voigt T, Chen Z, Mayr M, Karim R, Rhode K, et al. Native T1 Mapping in Differentiation of Normal Myocardium From Diffuse Disease in Hypertrophic and Dilated Cardiomyopathy. JACC: Cardiovascular Imaging. 2013; 6: 475-484.

51. Liu CY, Bluemke DA, Gerstenblith G, Zimmerman SL, Li J, Zhu H, et al. Reference Values of Myocardial Structure, Function, and Tissue Composition by Cardiac Magnetic Resonance in Healthy African-Americans at 3T and Their Relations to Serologic and Cardiovascular Risk Factors. The American Journal of Cardiology. 2014; 114: 789-795.

52. Bull S, White SK, Piechnik SK, Flett AS, Ferreira VM, Loudon M, et al. Human non-contrast T1 values and correlation with histology in diffuse fibrosis. Heart. 2013; 99: 932-937.

53. Karamitsos TD, Piechnik SK, Banypersad SM, Fontana M, Ntusi NB, Ferreira VM, et al. Noncontrast T1 Mapping for the Diagnosis of Cardiac Amyloidosis. JACC: Cardiovascular Imaging, 2013; 6: 488-497.

54. Dall'Armellina E, Piechnik S, Ferreira V, Quang Le Si, Matthew D Robson, Jane M Francis, et al. Cardiovascular magnetic resonance by non contrast T1-mapping allows assessment of severity of injury in acute myocardial infarction. Journal of Cardiovascular Magnetic Resonance. 2012; 14: 15.

55. Messroghli DR, Walters K, Plein S, Sparrow P, Friedrich MG, Ridgway JP, et al. Myocardial T1 mapping: Application to patients with acute and chronic myocardial infarction. Magnetic Resonance in Medicine. 2007; 58: 34-40.

56. Giri S, Chung YC, Merchant A, Mihai G, Rajagopalan S, Raman SV, et al. T2 quantification for improved detection of myocardial edema. Journal of Cardiovascular Magnetic Resonance. 2009; 11: 56.

57. Carlsson M, Martin AJ, Ursell PC, Saloner D, Saeed M. Magnetic resonance imaging quantification of left ventricular dysfunction following coronary microembolization. Magnetic Resonance in Medicine. 2009; 61: 595-602.

58. Carlsson M, Wilson M, Martin AJ, Saeed M. Myocardial Microinfarction after Coronary Microembolization in Swine: MR Imaging Characterization. Radiology. 2009; 250: 703-713.

59. Suhail MS, Wilson MW, Hetts SW, Saeed M. Magnetic resonance imaging characterization of circumferential and longitudinal strain under various coronary interventions in swine. World Journal of Radiology. 2013; 5: 472-483.

60. Monreal G, Gerhardt MA, Kambara A, Abrishamchian AR, Bauer JA, Goldstein AH, et al. Selective microembolization of the circumflex coronary artery in an ovine model: Dilated, ischemic cardiomyopathy and left ventricular dysfunction. Journal of Cardiac Failiur. 2004; 10: 174-183.

61. Ma J, Qian J, Ge J, Zeng X, Sun A, Chang S, et al. Changes in left ventricular ejection fraction and coronary flow reserve after coronary microembolization. Archives of Medical Science: AMS. 2012; 8: 63-69.

62. Ma J, Qian J, Chang S, Chen Z, Jin H, Zeng M. et al. Left ventricular remodeling with preserved function after coronary microembolization: the effect of methylprednisolone. European Journal of Medical Research. 2014; 19: 7.

63. Cimino S, Canali E, Petronilli V, et al. Global and regional longitudinal strain assessed by two-dimensional speckle tracking echocardiography identifies early myocardial dysfunction and transmural extent of myocardial scar in patients with acute ST elevation myocardial infarction and relatively. European Heart Journal - Cardiovascular Imaging. 2013; 14: 805-811.

64. Galiuto L. Optimal therapeutic strategies in the setting of post-infarct no reflow: the need for a pathogenetic classification. Heart. 2004; 90: 123-125.

65. Jain A, Mahmarian JJ, Borges-Neto S, Johnston DL, Cashion WR, Lewis JM, et al. Clinical significance of perfusion defects by thallium-201 single photon emission tomography following oral dipyridamole early after coronary angioplasty. Journal of American College of Cardiology. 1988; 11: 970-976.

66. Hardoff R, Shefer A, Gips S, Merdler A, Flugelman MY, Halon DA, et al. Predicting late restenosis after coronary angioplasty by very early (12 to 24 h) thallium-201 scintigraphy: implications with regard to mechanisms of late coronary restenosis. Journal of American College of Cardiology. 1990; 15: 1486-1492.

67. Skyschally A, Leineweber K, Gres P, et al. Coronary microembolization. Basic Research Cardiology, 2006; 101: 373-382.

68. Skyschally A, Schulz R, Erbel R, Heusch G. Reduced coronary and inotropic reserves with coronary microembolization. American Journal of Physiology Heart Circ Physiol. 2002; 282: H611-H614.

69. Carlsson M, Wilson M, Martin AJ, Saeed M. Myocardial microinfarction after coronary microembolization in swine: MR imaging characterization. Radiology. 2009; 250: 703-713.

70. Selvanayagam JB, Cheng AS, Jerosch-Herold M, Rahimi K, Porto I, van Gaal W, et al. Effect of distal embolization on myocardial perfusion reserve after percutaneous coronary intervention: a quantitative magnetic resonance perfusion study. Circulation. 2007; 116: 1458-1464.

71. Mohlenkamp S, Beighley PE, Pfeifer EA, Behrenbeck TR, Sheedy PF 2nd, Ritman EL. Intramyocardial blood volume, perfusion and transit time in response to embolization of different sized microvessels. Cardiovascular Research. 2003; 57: 843-852.

72. Bai Y, Hu L, Yu D, Peng S, Liu X, Zhang M et al. Evolution of Coronary Flow in an Experimental Slow Flow Model in Swines: Angiographic and Pathological Insights. BioMed Research International. 2015; 2015: 623986.

73. Saeed M, Hetts SW, English J, Do L, Wilson MW. Quantitative and qualitative characterization of the acute changes in myocardial structure and function after distal coronary microembolization using MDCT. Academic Radiology. 2011; 18: 479-487.

74. Jablonowski R, Wilson MW, Joudi N, Hetts SW, Saeed M. Three-dimensional MRI Assessments of Patchy and Large Myocardial Infarction in Beating and Nonbeating Swine Hearts: Validation with Microscopy. Academic Radiology. 2014; 21: 1048-1055.

75. Jablonowski R, Wilson MW, Do L, Hetts SW, Saeed M. Multidetector CT Measurement of Myocardial Extracellular Volume in Acute Patchy and Contiguous Infarction: Validation with Microscopic Measurement. Radiology. 2015; 274: 370-378.

76. Malyar NM, Gossl M, Beighley PE, Ritman EL. Relationship between arterial diameter and perfused tissue volume in myocardial microcirculation: a micro-CT-based analysis. American Journal of Physiology Heart Circulation Physiology. 2004; 286: H2386-H2392.

77. Weihrauch D, ZR, Arras M, Schaper J. Expression of extracellular matrix proteins and the role of fibroblasts and macrophages in repair processes in ischemic porcine myocardium. Cellular and Molecular Biological Research. 1994; 40: 105-116.

78. Nahrendorf M, Swirski FK, Aikawa E, Stangenberg L, Wurdinger T, Figueiredo JL, et al. The healing myocardium sequentially mobilizes two monocyte subsets with divergent and complementary functions. The Journal of Experimental Medicine. 2007; 204: 3037-3047.

79. Frangogiannis NG. The Mechanistic Basis of Infarct Healing. Antioxidants and Redox Signaling. 2006; 8: 1907-1939.

80. Nahrendorf M, Pittet MJ, Swirski FK. Monocytes: Protagonists of Infarct Inflammation and Repair After Myocardial Infarction. Circulation. 2010; 121: 2437-2445.

81. Frantz S, Nahrendorf M. Cardiac macrophages and their role in ischaemic heart disease. Cardiovascular Research. 2014; 102: 240-248.

82. Wang C, Wang SX, Dong PS, Wang LP, Duan NN, Wang YY, et al. Pathological observation of acute myocardial infarction in Chinese miniswine. International Journal of Clinical and Experimental Medicine. 2015; 8: 20829-20836.

83. Bonaventura A, Montecucco F, Dallegri F. Cellular recruitment in myocardial ischaemia/reperfusion injury. Eurean Journal of Clinical Investigation. 2016; 46: 590-601.

84. Alam SR, Shah ASV, Richards J, Lang NN, Barnes G, Joshi N, et al. Ultrasmall Superparamagnetic Particles of Iron Oxide in Patients With Acute Myocardial Infarction: Early Clinical Experience. Circulation: Cardiovascular Imaging. 2012; 5: 559-565.

85. Wollenweber T, Roentgen P, Schafer A, Schatka I, Zwadlo C, Brunkhorst T, et al. Characterizing the inflammatory tissue response to acute myocardial infarction by clinical multimodality noninvasive imaging. Circulation Cardiovascular Imaging. 2014; 7: 811-8.

86. Frangogiannis NG. Regulation of the inflammatory response in cardiac repair. Circulation Research. 2012; 110: 159-173.

87. Saeed M, Bajwa HZ, Do L, Hetts SW, Wilson MW. Multi-detector CT and MRI of microembolized myocardial infarct: monitoring of left ventricular function, perfusion, and myocardial viability in a swine model. Acta Radiologica. 2016; 57: 215-224.

88. Kloner RA. No-Reflow Phenomenon: Maintaining Vascular Integrity. Journal of Cardiovascular Pharmacology and Therapeutics. 2011; 16: 244-250.

89. Wu KC. CMR of microvascular obstruction and hemorrhage in myocardial infarction. Journal of cardiovascular magnetic resonance. 2012; 14: 68.

90. Ertl G, Frantz S. Healing after myocardial infarction. Cardiovascular Research. 2005; 66: 22-32.

91. Lund GK, Stork A, Muellerleile K, Barmeyer AA, Bansmann MP, Knefel M, et al. Prediction of left ventricular remodeling and analysis of infarct resorption in patients with reperfused myocardial infarcts by using contrast-enhanced MR imaging. Radiology. 2007;245: 95-102.

92. Saeed M, Lee RJ, Weber O, Do L, Martin A, Ursell P, et al. Scarred myocardium imposes additional burden on remote viable myocardium despite a reduction in the extent of area with late contrast MR enhancement. Eurpean Radiology. 2006; 16: 827-836.

93. Choi CJ, Haji-Momenian S, Dimaria JM, Epstein FH, Bove CM, Rogers WJ, et al. Infarct involution and improved function during healing of acute myocardial infarction: the role of microvascular obstruction. Journal Cardiovascular Magnetic Resononance. 2004; 6: 917-925.

94. Ingkanisorn WP, Rhoads KL, Aletras AH, Kellman P, Arai AE. Gadolinium delayed enhancement cardiovascular magnetic resonance correlates with clinical measures of myocardial infarction. Journal of the American College of Cardiology. 2004; 43: 2253-2259.

95. Grutzendler J, Murikinati S, Hiner B, Ji L, Lam CK, Yoo T, et al. Angiophagy Prevents Early Embolus Washout But Recanalizes Microvessels Through Embolus Extravasation. Science Translational Medicine. 2014; 6: 226ra31.

96. Lam CK, Yoo T, Hiner B, Liu Z, Grutzendler J. Embolus extravasation is an alternative mechanism for cerebral microvascular recanalization. Nature. 2010; 465: 478-482.

97. Chen Z, Qian J, Ma J, Chang S, Yun H, Jin H, et al. Glucocorticoid ameliorates early cardiac dysfunction after coronary microembolization and suppresses TGF-β1/Smad3 and CTGF expression. International Journal of Cardiology. 2013; 167: 2278-2284.

98. Jin H, Yun H, Ma Jy, Chen ZW, Chang SF, Ge MY, et al. Assessment of the acute effects of glucocorticoid treatment on coronary microembolization using cine, first-pass perfusion, and delayed enhancement MRI. Journal of Magnetic Resonance Imaging. 2016; 43: 921-928.

99. Hori M, Gotoh K, Kitakaze M, Iwai K, Iwakura K, Sato H, et al. Role of oxygen-derived free radicals in myocardial edema and ischemia in coronary microvascular embolization. Circulation. 1991; 84: 828-840.

100. Cai Z, Semenza GL. PTEN Activity Is Modulated During Ischemia and Reperfusion: Involvement in the Induction and Decay of Preconditioning. Circulation Research. 2005; 97: 1351-1359.